Glucagon regulates intracellular distribution of adipose differentiation-related protein during triacylglycerol accumulation in the liver[S]

Katsuhiko Takahashi,[1,*] Naoko Sasabe,[*] Kumiko Ohshima,[*] Keiko Kitazato,[*,§] Rina Kato,[*] Yutaka Masuda,[†] Mika Tsurumaki,[*] Takashi Obama,[*] Shin-ichi Okudaira,[**] Junken Aoki,[**] Hiroyuki Arai,[††] Tomohiro Yamaguchi,[*] and Hiroyuki Itabe[2,*]

Department of Biological Chemistry,* School of Pharmacy, Showa University, Tokyo, Japan; Department of Neuronal Surgery,§ Institute of Health Biosciences, University of Tokushima Graduate School, Tokushima, Japan; Department of Molecular Cellular Pathophysiology,† Showa Pharmaceutical University, Tokyo, Japan; Department of Molecular and Cellular Biochemistry,** Graduate School of Pharmaceutical Sciences, Tohoku University, Miyagi, Japan; and Department of Health Chemistry,†† Graduate School of Pharmaceutical Sciences, University of Tokyo, Tokyo, Japan

Abstract Cellular lipid droplets (LD) are organelles involved in cellular lipid metabolism. When liver cellular components were fractionated using sucrose density gradient centrifugation, adipose differentiation-related protein (ADRP) was distributed in both the top and bottom fractions, which correspond to the LD and membranous fractions, respectively, in the mouse liver under normal feeding conditions. After overnight fasting, triacylglycerol and ADRP increased nearly 2.5-fold in the mouse liver, and a portion appeared in the intermediate-density LD (iLD) fractions. ADRP in the iLD fractions was also increased in a mouse nonalcoholic steatohepatitis model induced by methione/choline-deficient diet. When HuH-7 human hepatoma cells were incubated with oleic acid for 24 h, the amount of ADRP increased, and it was distributed in both the LD and membrane fractions. However, ADRP appeared in the iLD fractions upon treatment of HuH-7 cells with glucagon. This behavior of ADRP was cAMP-dependent, as the ADRP-positive iLD fractions were induced by dibutylyl cAMP and were blocked by protein kinase A inhibitors. A portion of ADRP colocalized microscopically with calnexin, which is present in the iLD fractions, by treatment of HuH-7 cells or human primary hepatocytes with oleic acid and glucagon, but not by treatment with oleic acid alone. Glucagon has a role in the reorganization of endoplasmic reticulum membranes to generate ADRP-associated lipid-poor particles in hepatic cells, which is related to LD formation during lipid storage.— Takahashi, K., N. Sasabe, K. Ohshima, K. Kitazato, R. Kato, Y. Masuda, M. Tsurumaki, T. Obama, S-i. Okudaira, J. Aoki, H. Arai, T. Yamaguchi, and H. Itabe. **Glucagon regulates intracellular distribution of adipose differentiation-related protein during triacylglycerol accumulation in the liver. *J. Lipid Res.* 2010.** 51: **2571–2580.**

Supplementary key words fatty liver • hepatocytes • HuH-7 • lipid droplets • NASH • phospholipase C • protein kinase A • sucrose density gradient centrifugation

Intracellular lipid droplets (LD) are cellular organelles observed ubiquitously in physiological and pathological conditions. LDs are composed of a core of neutral lipids containing cholesteryl esters and/or triacylglycerol (TG), a surrounding surface monolayer of phospholipids, and several associated proteins. LDs are considered to be a storage site of neutral lipids and to play a role in whole-body energy homeostasis (1–3).

A number of proteomic studies on LD in various cells have revealed the unique protein profiles of LD (4–8). A

Abbreviations: Ab, antibody; ADRP, adipose differentiation-related protein; ER, endoplasmic reticulum; GRP78/BiP, glucose-regulated protein of 78-kDa/binding protein; iLD, intermediate-density lipid droplet; LD, lipid droplet; MCD, methione/choline deficient; MTP, microsomal triacylglycerol transfer protein; NASH; nonalcoholic steatohepatitis; OA, oleic acid; PAT, perilipin-ADRP-TIP47; PLP, 4% paraformaldehyde-lysine-sodium periodate; PC, phosphatidylcholine; PKA, protein kinase A; PKI, PKI14-22amide; PLC, phospholipase C; PNS, post-nuclear supernatant; PPAR, peroxisome proliferator-activated receptor; Rp, Rp-8-Br-cAMPS; SCD-1, stearoyl-CoA desaturase-1; TG, triacylglycerol; TIP47; tail interacting protein of 47 kDa; WAT, white adipose tissue.

[1] Present address of K. Takahashi: Physiological Chemistry Research Laboratory, Institute of Medicinal Chemistry, Hoshi University, Shinagawa-ku, Tokyo 142-8501, Japan.

[2] To whom correspondence should be addressed.
e-mail: h-itabe@pharm.showa-u.ac.jp

[S] The online version of this article (available at http://www.jlr.org) contains supplementary data in the form of four figures.

This work was supported in part by grants-in-aid from the Ministry of Education, Culture, Sports, Science, and Technology (MEXT) of Japan; by a grant for Research on Publicly Essential Drugs and Medical Devices from the Japan Health Science Foundation; and by the High-Tech Research Center Project for Showa University (matching fund subsidy from MEXT, 2005–2009).

Manuscript received 7 December 2009 and in revised form 6 June 2010.

Published, JLR Papers in Press, June 6, 2010
DOI 10.1194/jlr.M004648

well-known family of LD-associated proteins is the PAT family, which includes adipose differentiation-related protein (ADRP, also called adipophilin or ADFP), perilipin, tail interacting protein of 47 kDa (TIP47), myocardial lipid droplet protein (MLDP, also called OXPAT or LPDP5), and S3-12 (9, 10). These proteins share the PAT domain, which is named after the three major family members: perilipin, ADRP, and TIP47 (7). Perilipin is a specialized LD protein expressed in mature adipocytes, and it has a pivotal role in the regulation of TG hydrolysis in cells (11, 12). Hormone-induced TG hydrolysis is regulated by protein kinase A (PKA)-dependent phosphorylation of hormone-sensitive lipase (HSL) and perilipin. In unstimulated cells, perilipin forms a complex with comparative gene identification-58 (CGI-58), but phosphorylated perilipin dissociates from CGI-58, and then the CGI-58 binds to adipose triglyceride lipase (ATGL) to activate the enzyme. Phosphorylated perilipin facilitates the access of phosphorylated HSL to the surface of LD, and hydrolyzes the diacylglycerol formed from TG by ATGL (13–15).

ADRP was originally found as a major protein induced in the early stages of 3T3-L1 adipocyte differentiation (16). The expression of *Adrp* mRNA is induced not only in adipocytes but also in many other types of cells upon lipid accumulation (17–21). It is reported that peroxisome-proliferator activated protein (PPAR)-retinoid X receptor (RXR) heterodimers are responsible for ADRP transcription, while PPARγ is the major subtype in adipose tissue and the placenta (22, 23), PPARδ is crucial in macrophages (19), and PPARα acts in the liver (20, 24).

It is well known that ADRP is an LD-associated protein expressed in many cell types, and it is widely used as a marker of LD. However, the behavior and biological roles of ADRP remain to be investigated. One of the difficulties in studying the behavior of ADRP is that the protein level is not necessarily dependent on the mRNA level. Previous in vitro studies have shown that ADRP is involved in LD formation by enhancing the uptake of free fatty acids (FFA), thereby stabilizing LD particles (25, 26). Recently, we and another group found that the ubiquitin-proteasome system regulates the ADRP level during the regression of lipid-accumulating cells, and it was apparent that ADRP escaped from the degradation system during LD formation (21, 27). In addition, the intracellular distribution of ADRP changed under various conditions. ADRP does not contain a signal sequence or transmembrane domain, so it is unlikely to be produced by membrane-bound ribosomes on rough endoplasmic reticulum (ER); rather, it may move between the cytosol and the LD surface after translation. We thought that monitoring the changes in the amount and distribution of ADRP would provide new insight into the biological functions of ADRP.

In the current study, we found the formation of intermediate density LDs (iLD) in the liver that contain ADRP but are poor in TG. Induction of the iLD fraction is observed during lipid accumulation in the fasted liver and in a dietary murine model of nonalcoholic steatohepatitis (NASH). We investigated the factors responsible for appearance of ADRP-positive iLD fractions using the hepatoma cell line HuH-7, and we found that glucagon induces the change in ADRP distribution. This response was mediated by PKA-dependent signaling pathway. These observations suggest the novel idea that the intracellular distribution of ADRP to the iLD fraction is hormonally regulated and could be coupled with LD particle formation during lipid loading in the liver.

EXPERIMENTAL PROCEDURES

Animals

Male C57BL6/J mice (10 weeks old) purchased from Oriental Yeast Co. (Tokyo, Japan) were maintained in a temperature-controlled facility with fixed 12 h light and 12 h dark cycles and free access to regular chow and water. Animals from 10 to 12 weeks of age were used throughout this study unless otherwise indicated. For the fasting experiment, diet was withdrawn from the mice for 16 h. For the NASH experiment, mice were fed a methionine/choline-deficient (MCD) diet (CLEA Japan, Tokyo, Japan) for 2 weeks (28, 29).

Subcellular fractionation

Subcellular fractionation of the mouse liver was carried out by sucrose density gradient ultracentrifugation. Briefly, the dissected tissues were disrupted by homogenization with a Teflon/glass homogenizer in isotonic buffer [5 mM Tricin-NaOH (pH 7.4), 0.75 mM EDTA, 250 mM sucrose, and a protease inhibitor cocktail]. The homogenate was centrifuged at 10,000 *g* for 5 min at 4°C, yielding a postnuclear supernatant (PNS). The sucrose concentration of the PNS was adjusted to 35% and layered beneath a 2–35% sucrose gradient. The ultracentrifugation was carried out at 154,000 *g* for 2 h at 4°C using an RPS40T rotor and a Himac CP65β ultracentrifuge (Hitachi, Japan). Following centrifugation, the samples were collected from the top (0.8 ml each), and 13 (liver PNS samples) or 15 (HuH-7 PNS samples) fractions were recovered. The density of each fraction was determined using a multi-wavelength Abbe refractometer (Atago Co. Ltd.).

Cell culture experiments

Human hepatoma cell line HuH7 was purchased from RIKEN Health Research Resource Bank. Cells were grown in DMEM containing 10% FBS, 200 mM L-glutamine, 100 U/ml penicillin, and 100 μg/ml streptomycin. Cells were incubated with the medium supplemented with 0.6 mM oleic acid (OA) and/or 100 nM glucagon (Sigma, St. Louis, MO) for 24 h. Then the cells were collected using a cell scraper and homogenized in isotonic buffer using a glass homogenizer. After centrifugation at 10,000 rpm for 5 min at 4°C, the recovered supernatant was used as PNS. Human primary hepatocytes were purchased from BD Biosciences, San Jose, CA (cat. no. 454550; lot no. 262). The hepatocytes were washed with ISOM's medium, and then cultured in ISOM's medium containing 10% FBS for 12 h, followed by 2 days culture in ISOM's medium without FBS according to the manufacture's instruction. Then the cells were incubated with DMEM supplemented with 0.6 mM OA and 100 nM glucagon for 24 h.

Immunoblot analysis

Total lysates from the dissected murine tissues were prepared with SDS/Triton X-100 lysis buffer [50 mM Tris-HCl (pH 7.5), 0.1% SDS, 1% Triton X-100, 1 mM EDTA, 150 mM NaCl, and a protease inhibitor cocktail (Sigma)]. Protein concentrations of the total lysates were measured using the BCA protein assay reagent (Pierce). Aliquots of the total lysates were subjected to 10%

SDS-PAGE, and then transferred to nitrocellulose membranes (Protron BA-83; Schleicher and Schuell). The membranes were probed with specific antibodies against mouse ADRP (Progen, Heidelberg, Germany); human ADRP (American Research Products); stearoyl-CoA desaturase (SCD-1; Santa Cruz); glucose-regulated protein of 78 kDa (GRP78/BiP; BD Biosciences), TIP47 (Santa Cruz); perilipin (Progen); microsomal triacylglycerol transfer protein (MTP; BD Biosciences); Raf-1 and enolase (Santa Cruz); calnexin and mouse β-actin (Sigma); and human β-actin (Santa Cruz). Proteins were visualized using the ECL-plus system (Invitrogen, Carlsbad, CA).

Microscopic examinations

HuH-7 cells (5×10^4 cells/ml) cultured in Lab-Tek II slide chambers (Nalge Nunc International) were treated with or without OA (0.6 mM) and glucagon (100 nM) for 24 h. The cells were fixed with 10% formalin-PBS for 10 min at room temperature. The cells were then permeabilized and blocked by treatment with PBS containing 0.2 M glycine and 0.1 mg/ml saponin for 45 min, followed by PBS containing 20 μg/ml nonimmune goat IgG and 0.1 mg/ml saponin for 1 h. The cells were incubated with anti-ADRP guinea pig IgG (Progen), anti-calnexin rabbit IgG (Sigma), or anti-GRP78/BiP rabbit IgG (Sigma), followed by the mixture of second antibodies (biotin-conjugated anti-guinea pig IgG and Alexa594-streptavidine, Alexa488-anti rabbit IgG). LDs were stained with BODIPY493/503 (Molecular Probes). The cells were observed and photographed using confocal laser microscopy (Nikon A1-si).

Measurement of particle sizes

Fractions recovered from sucrose density gradient ultracentrifugation were diluted 1:10 with buffer A [10 mM Tricine-NaOH (pH 7.4) containing 3 mM EDTA]. The average particle size in the fractions were measured using a laser diffraction nanoparticle size analyzer (Simadzu SALD-7100).

Measurement of TG and FFA

Mice were anesthesized and whole venous blood was obtained from the inferior vena cava. The amounts of TG and FFA in blood were determined using a Triglyceride E-Test and NEFA C-Test (Wako Chemical Co., Osaka, Japan).

Statistical analysis

Data are expressed as mean ± standard deviation. Results were analyzed using Student's *t*-test, and statistical significance for all comparisons were assigned at $P < 0.05$. Asterisks indicate values significantly different from the control: $*P < 0.05$, $**P < 0.01$, $***P < 0.005$.

RESULTS

Intracelluar distribution of ADRP protein

The ADRP protein was detected by immunoblotting in various tissues from 10-week-old, male C57BL/6 mice. The expression of ADRP was the highest in the liver (supplementary Fig. I), but ADRP was not detected in white adipose tissue (WAT). Perilipin was observed only in WAT among the tissues examined. Liver has a central role systemic lipid homeostasis, and we studied the behavior of the ADRP protein in liver cells during lipid accumulation.

Fasting induces mobilization of stored fat and accumulation of TG in the liver. When the blood glucose level decreases during the fasting period, glucagon stimulates glycogenolysis and adrenalin upregulates TG hydrolysis in WAT to increase the FFA released into the circulation, and then excess amounts of FFA are converted to TG in the liver (30, 31). After mice were fasted for 16 h, ADRP protein was increased in the liver of the fasted mice (2.6-fold) but not in the other tissues examined (**Fig. 1A**). This is in accordance with a previous report showing an increase in ADRP and TG in the fasted mouse liver (32). The amounts of TG in brain, heart, and muscle did not change significantly after 16 h of fasting (data not shown).

TIP47, another member of the PAT family of proteins, was also induced approximately 4.1-fold (Fig. 1B) in the fasted liver. In addition, an ER membrane protein, SCD-1, which has a key role in providing unsaturated fatty acids for utilization in TG production, was induced in the fasted liver (~2.7-fold), suggesting that substantial changes in the ER occur during TG accumulation in the liver.

To study the intracellular distribution of ADRP in the hepatic cells during TG accumulation, we examined the

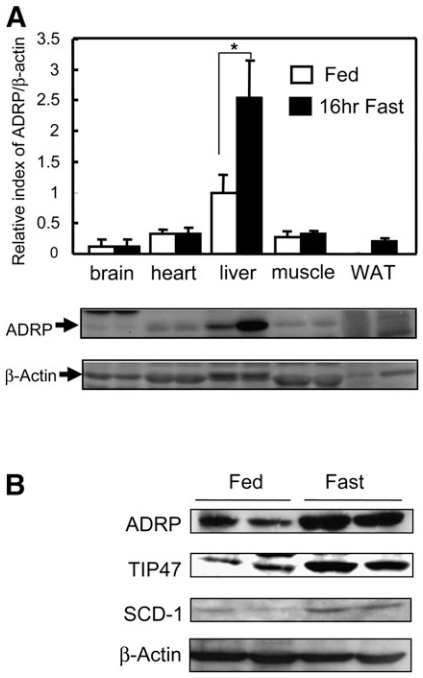

Fig. 1. Accumulation of ADRP in the liver of fasting mice. A: Effects of fasting on ADRP protein levels in the tissues were examined. Male C57BL/6 mice (10 weeks old) were either fed chow diet or fasted for 16 h, euthanized, and then brain, heart, liver, skeletal muscle, and WAT were recovered. Immunoblot analysis of ADRP protein levels in each type of mouse tissue was performed, and the intensity of the detected bands for ADRP and β-actin were quantified by densitometric scanning. The relative index of 1.0 is the ADRP/β-actin in the liver from chow-fed mice. Bar graph shows mean and standard deviation of three mice. B: Fasting altered levels of TIP47, another LD protein, and SCD-1, an enzyme involved in lipid metabolism. Among the PAT family proteins, perilipin was not detectable. The intensity of the detected bands of ADRP, TIP47, SCD-1, and β-actin were quantified by densitometric scanning. ADRP, adipose differentiation-related protein; LD, lipid droplet; SCD-1, stearoyl-CoA desaturase-1; TIP47; tail interacting protein of 47 kDa; WAT, white adipose tissue.

profiles of ADRP in the liver homogenates by sucrose density gradient centrifugation. The homogenate from the mice treated with a normal diet was separated into 13 fractions by density gradient. Because the liver PNS fraction was placed in the bottom of the tube before centrifugation, the bottom fractions (Fr. No. 12, 13) would be expected to contain most of the proteins and membranous organelles. As shown in **Fig. 2A**, two ER proteins, MTP and GRP78/BiP, and a cytosolic protein, Raf-1, were localized in the bottom fractions. ADRP was distributed in both the top (Fr. No. 1, 2) and bottom fractions (Fr. No. 12, 13) but not in the middle fractions (Fr. No. 5–9) (Fig. 2A, B), while TG was also mainly distributed in the top fractions (Fig. 2C). The mouse liver after 16 h fast displayed a massive accumulation of TG in the top fractions. A small but substantial increase in TG was found in the middle fractions, but no TG increase was observed in the bottom fractions (Fig. 2C). ADRP in the top fractions (Fr. No. 1–3) increased approximately 3-fold, and ADRP in the bottom fractions was also increased (Fig. 2A). It should be noted that significant amounts of ADRP appeared in the iLD fractions (Fr. No. 5–9) in the fasted mouse liver. The iLD fractions from the fasted mouse liver contained more TG than that from the fed mouse, suggesting dense, lipid-poor LD particles had formed in the fasted mouse liver. Although the distribution of Raf-1 remained unchanged, portions of MTP and GRP78/BiP were detected (Fr. No. 8–11). TIP47 was detected in the top fractions (Fr. No. 1, 2) of both the fed and fasted livers but not in the iLD fractions (Fig. 2A).

ADRP in a dietary murine model of NASH

Feeding mice with the MCD diet for more than one week induces strong accumulation of TG and tissue damage in the liver, a fact which is used in the experimental model of NASH (28, 29). When 10 week-old male mice were fed the MCD diet for two weeks, they exhibited a 4-fold increase in the ADRP level together with a 3-fold increase in TG level in the liver (**Fig. 3A-C**). Sucrose density gradient centrifugation of the liver PNS fractions from the mice fed with the MCD diet demonstrated that ADRP and TG were distributed in the iLD fractions (Fr. No. 5–9) in addition to a 3-fold increase in the top and bottom fractions (Fig. 3B-E). In the liver from control mice, TG was located in the top fractions (Fr. No. 1, 2) and ADRP was distributed in both the top and bottom fractions. The changes in the distribution pattern of ADRP and TG after MCD treatment are very similar to those observed in the fasting liver. From these results, it is likely that the ADRP-positive iLD fractions are induced in response to TG accumulation under pathological conditions, in addition to physiological metabolic changes.

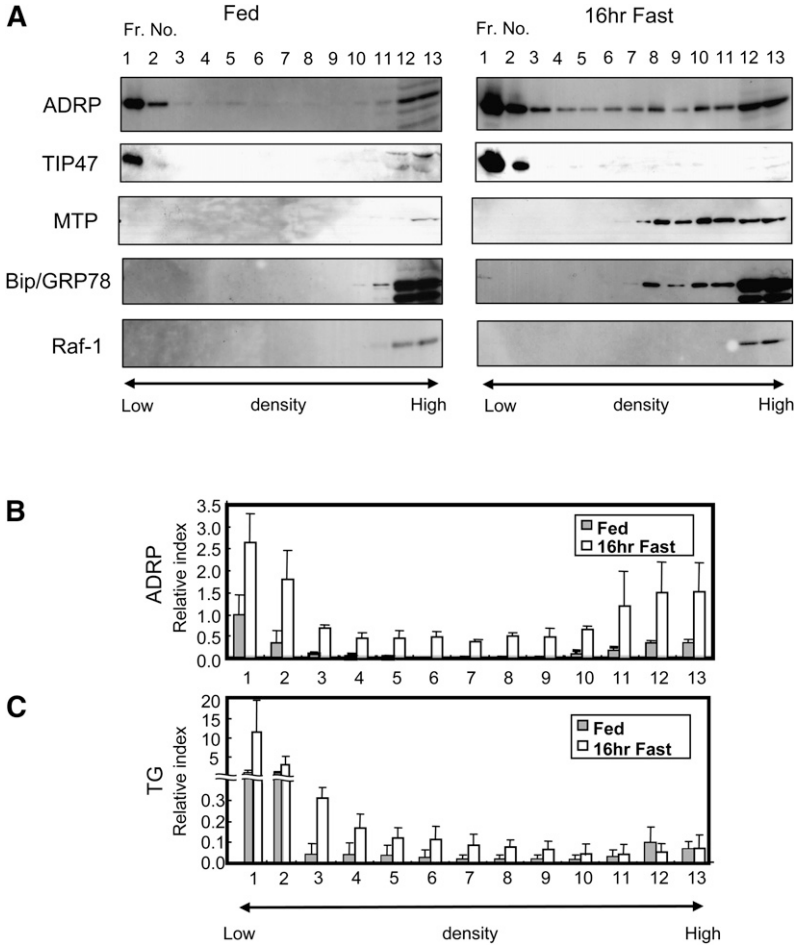

Fig. 2. ADRP-LDs with intermediate density appeared in the fasted liver. A: The profiles of ADRP, TIP47, MTP, GRP78/BiP, and Raf-1. The liver PNS fractions from mice under feeding conditions and after fasting for 16 h were fractionated by sucrose density gradient centrifugation. MTP and GRP78/BiP are marker proteins for ER; Raf-1 is a marker for cytosol. Each fraction from sucrose density gradient centrifugation was analyzed by immunoblot analysis. MTP seems to increase in the fasted liver, although we have not done a quantitative confirmation yet. B: Distribution of ADRP levels in the density gradient. The intensity of the detected bands of ADRP was quantified by densitometric scanning. The relative index of 1 is defined as the intensity of ADRP in fraction No. 1. C: Distribution of the TG levels in the density gradient. The TG levels of each fraction were quantitatively measured as described in "Experimental Procedures." The relative index of 1 is the TG level in fraction No. 1. ADRP, adipose differentiation-related protein; GRP78/BiP, glucose-regulated protein of 78-kDa/binding protein; LD, lipid droplet; MTP, microsomal triacylglycerol transfer protein; PNS, post-nuclear supernatant; TG, triacylglycerol; TIP47; tail interacting protein of 47 kDa.

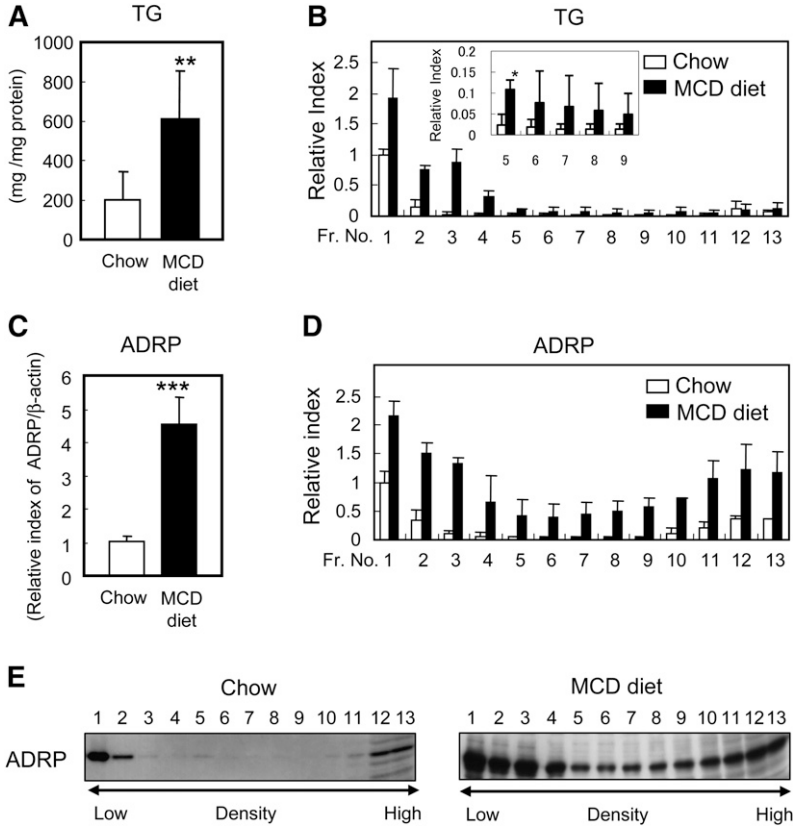

Fig. 3. Distribution of ADRP in iLD fractions in the MCD diet-induced fatty liver**.** Liver homogenates prepared from mice before and after feeding with the MCD diet for 2 weeks were fractionated using sucrose density gradient ultracentrifugation. A: TG levels in the liver homogenates were quantitatively measured by enzymatic assay. B: Distribution of TG in the liver. The TG levels in each fraction were measured. The inset shows detailed pattern of TG distribution in iLD fractions. C: ADRP and GAPDH in the liver homogenates were detected using immunoblot analysis. D, E: Distribution of ADRP after the fractionation was analyzed by immunoblot, and the band intensity was quantified by densitometric scanning (n = 3). The relative index of 1 is defined as the ADRP/GAPDH ratio in the livers of control mice (0-week treatment). $*P < 0.05$, $**P < 0.01$, $***P < 0.005$. ADRP, adipose differentiation-related protein; iLD, intermediate-density lipid droplet; MCD, methione/choline deficient; TG, triacylglycerol.

Induction of ADRP-associated iLD fractions in HuH-7 human hepatic cells

To elucidate the mechanisms involved in the distribution of ADRP to the iLD fractions, the distribution of ADRP was investigated in hepatic cells in culture. Human hepatoma cell line HuH-7 is widely used in studies of lipid metabolism related to LD and/or lipoprotein metabolism (5, 33–35). After HuH-7 cells were incubated with OA for 24 h to induce intracellular LDs, the cell lysate was separated by sucrose ultracentrifugation. Compared with cells without the OA treatment, the amounts of ADRP did not increase, although TG increased 2.5-fold, (**Fig. 4A**, B). Under both conditions, most of the ADRP was localized in the top fractions (Fr. No. 1, 2) (Fig. 4D). Such distribution patterns of ADRP and TG in OA-treated HuH-7 cells do not correspond to those observed in the fasted liver and the MCD-induced fatty liver, suggesting that factors other than fatty acids are involved in formation of iLD fractions in hepatocytes, even though fatty acid is sufficient to induce the accumulation of buoyant LDs.

During fasting, the blood sugar level decreases, and the energy supply is shifted from a glycolysis-dependent system to a fatty acid-dependent metabolism. Under such conditions, in addition to mobilization of FFA into the blood stream, the glucagon level increases to stimulate glycogenolysis. When HuH-7 cells were incubated with glucagon in the presence of OA for 24 h, ADRP was distributed in the iLD and bottom fractions (Fig. 4A). Interestingly, treatment of the cells with glucagon alone was sufficient to induce the distribution of ADRP to the iLD fractions, although the addition of glucagon had no effect on the amounts of ADRP and TG (Fig. 4A, B). Treatment of the cells with glucagon with OA changed the distribution of both ADRP and TG, suggesting that the iLD fractions contained a small but definite amount of TG (Fig. 4D, E). The effect of glucagon on the TG increase was most potent in the iLD fractions (Fig. 4C).

The intracellular distributions of enolase, GRP78/BiP, and calnexin in the cells treated with both OA and glucagon were studied (**Fig. 5A**). Enolase, a cytosolic enzyme involved in glycolysis, was found in the bottom fractions. GRP78/BiP was found in the bottom fractions and in part in the top fraction, which corresponds to the data from the fasted liver and fatty liver models. Interestingly, calnexin showed a wide distribution from the top to the bottom, with a considerable amount detected in the iLD fractions either with or without OA and glucagon OA treatment (Fig. 5A, B).

The distribution of ADRP in HuH-7 cells was examined under confocal laser microscopy. When HuH-7 cells were treated with OA, relatively large LD particles surrounded by ADRP were induced. After treatment with OA and glucagon, both large and small LD particles, which were surrounded by ADRP, were observed (**Fig. 6A**). The staining patterns of calnexin and GRP78/BiP corresponded to those of ER, with dense staining surrounding the nucleus and the reticular network all over the cytoplasmic space. Note that a part of calnexin, but not GRP78/BiP, colocalized with ADRP when the cells were treated with OA and glucagon (Fig. 6B, C), which correlates with the result

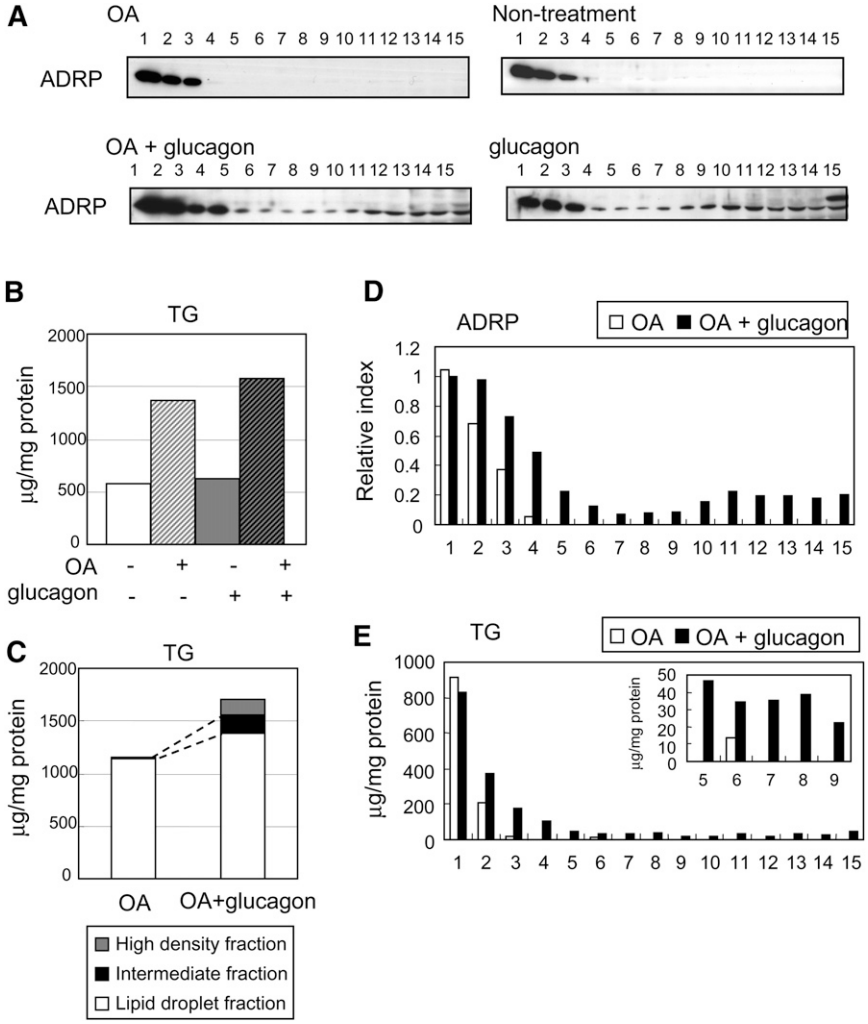

Fig. 4. ADRP appearance in the iLD fractions were induced by glucagon in HuH-7 human hepatoma cells. A: HuH-7 cells were incubated with or without 0.6 mM OA for 24 h, and in another set of cells, 100 nM glucagon was added for 24 h. Then the cell lysate was fractionated by sucrose ultracentrifugation. The same volume (8 µl) from each fraction was applied to SDS-PAGE and immunoblotted with anti-ADRP antibody. B: HuH-7 cells were treated as above, and the amount of TG in the cell lysates was measured. C: Distribution of TG in the cells incubated with OA with or without glucagon was assessed by dividing them into three fractions: LD fractions (Fr. No. 1–3), iLD fractions (Fr. No. 5–9), and high-density fractions (Fr. No. 11–15). D, E: Distribution of ADRP and TG in the cells incubated with OA with or without glucagon in each fraction separated by sucrose ultracentrifugation. The intensity of the detected bands of ADRP was quantified by densitometric scanning. The relative index of 1 is defined as the intensity of ADRP in fraction No. 1 from the HuH-7 cells treated with OA and glucagon. ADRP, adipose differentiation-related protein; iLD, intermediate-density lipid droplet; OA, oleic acid; TG, triacylglycerol.

of the sucrose density gradient centrifugation (Fig. 5). Enolase did not colocalize with ADRP under either condition (Fig. 6D).

Because hepatoma cell lines, such as HuH-7, might differ from the hepatocytes, the effects of OA and glucagon were also examined in human hepatocytes. The human hepatocytes accumulated a number of LD particles when incubated with OA or OA with glucagon (**Fig. 7A**). Colocalization of a part of ADRP with calnexin after treatment with glucagon and OA was again observed in the primary hepatocytes, while treatment of the hepatocytes with OA alone induced LDs, but the distribution of ADRP did not overlapped with calnexin (Fig. 7B, C).

Under our experimental conditions, the iLDs (Fr. No. 5–8) have a density between 1.05 and 1.10 (supplementary Fig. II). Considering that the density of plasma LDL (d = 1.019–1.063) and HDL (d = 1.063–1.215), the iLD fractions are likely to contain neutral lipid-poor particles. By using a laser diffraction nanoparticle-size analyzer, the average particle size in the iLD fractions was estimated to be approximately 0.5 µm (supplementary Fig. III). It is interesting that the estimated particle size seems to be even larger than the LDs in the top fractions.

Induction of ADRP-positive iLD fractions was observed after 5 h treatment of HuH-7 cells with OA and glucagon for 5 h, but 1 h treatment did not change the ADRP distribution (supplementary Fig. IV).

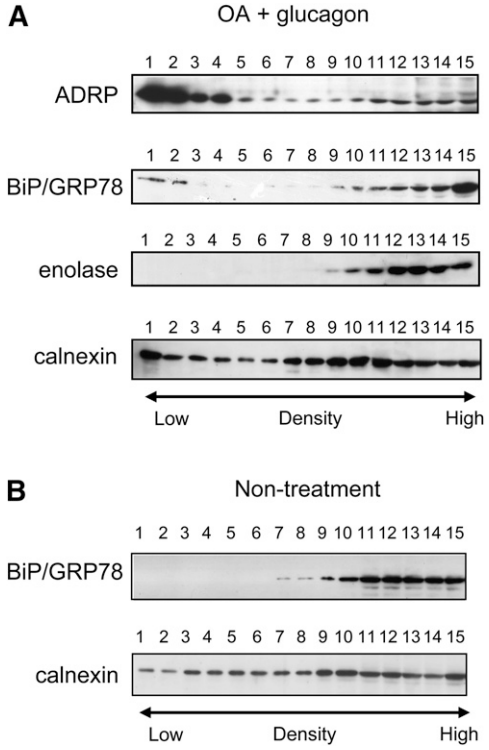

Fig. 5. Distribution of ADRP and other proteins in HuH-7 cells after incubation with OA and glucagon. A: HuH-7 cells were incubated with OA (0.6 mM) and glucagon (100 nM) for 24 h. Then the cell lysate was fractionated by sucrose ultracentrifugation, and the distribution of ADRP, enolase, BiP/GRP78, and calnexin were examined by Western blotting. B: Lysate of HuH-7 cells without treatment with OA and glucagon was fractionated by sucrose ultracentrifugation, and the distribution of BiP/GRP78, and calnexin were examined by Western blotting. ADRP, adipose differentiation-related protein; GRP78/BiP, glucose-regulated protein of 78-kDa/binding protein; OA, oleic acid.

Signaling pathway inducing ADRP redistribution

Since glucagon treatment of HuH-7 cells mobilized ADRP, the involvement of signaling pathways following glucagon receptor was studied. Treatment of HuH-7 cells with dibutylyl cAMP (db-cAMP) for 24 h induced ADRP distribution in the iLD fractions, just as glucagon did (**Fig. 8A**). The appearance of ADRP in the iLD fractions by either glucagon or db-cAMP was diminished in the presence of the PKA inhibitor Rp-8-Br-cAMPS (8-bromoadenosine-3',5'-cyclic monophosphothioate; Rp) or PKI14-22amide (PKI) (Fig. 8B). These results indicate that the redistribution of ADRP is induced, at least in part, through the PKA pathway. It was recently reported that the glucagon receptor couples with the Gq as well as Gs proteins (36). The distribution of ADRP in the iLD fractions in glucagon-treated HuH-7 cells was also abolished in the presence of the phospholipase C (PLC) inhibitor U-73122 (Fig. 8C).

DISCUSSION

In the present study, it was demonstrated that ADRP-associated iLDs were formed in hepatic cells during TG accumulation under physiological and pathological conditions and that this change in distribution of ADRP was mediated by glucagon. Although fatty acid availability is crucial for the increase of the ADRP mass, the glucagon-dependent distribution of ADRP to the iLD fractions was regulated differently.

In sucrose density ultracentrifugation of the PNS fraction from the fasted liver, we found that ADRP appeared in the iLD fractions. As the increase in ADRP is more obvious than the increase in TG in these fractions, ADRP is likely to form dense LD particles with a smaller amount of TG. Microscopic examination of the intracellular distribution of calnexin revealed an ER-like pattern, and glucagon treatment induced a portion of ADRP to colocalize with calnexin, which corresponds well with the presence of these proteins in iLD fractions in the cells treated with OA and glucagon. The different responses of calnexin and GRP78/BiP, the two ER proteins, suggest that there are subcompartments in ERs and iLDs that contain complex particles formed by nascent LDs and parts of ER membranes. It was proposed recently that LDs interact homotypically with other LD particles and heterotypically with other organelles (37). In particular, several recent studies have demonstrated a close association of LDs and ERs (38–41). Turró et al. reported a proteome study on hepatocytes showing calnexin was present as one of the associated proteins in the LD fraction (40). Recently, Fujimoto et al. proposed that LDs and ERs form complexes, which explains the unique structure called the "apoB crescent" (38, 39). Since our iLD fractions showed HDL-like density and much larger particle sizes, it is possible that there are LD-ER complexes like the apoB crescent in the iLD fractions.

The mechanisms for LD particle formation have not been fully clarified, but there is a strong suggestion that nascent LDs are derived from the ER membrane, because diacylglycerol acyltransferase, the enzyme involved in TG synthesis, is located on the ER membrane (1, 30). Using immunoelectron microscopic analysis, Robenek et al. demonstrated that ADRP was present in ER membranes of macrophages (41), and we observed that a substantial part of ADRP was present in the bottom fractions. It is possible that iLD particles are generated upon stimulation from the ER membranes. However, another possibility is that small iLD particles are present constitutively and ADRP accumulates in these particles upon stimulation. We cannot distinguish between these two possibilities currently because we do not have a distinct marker for iLDs. To answer this issue, further study on dynamic behavior of LDs and iLDs in the cells is needed. Note that there was a limitation of the sucrose density gradient method in separating iLD fractions and iLD/ER complex from the other cellular compartments. Proteome analysis as well as morphological examinations with electron microscopy would be useful to characterize the iLD fractions.

It is well known that the addition of fatty acid to various cells induces ADRP expression and LD formation and that PPAR-RXR heterodimers are involved in mRNA expression of the ADRP gene (19–25). We tested the effect of fatty acids on the distribution of ADRP using HuH-7 hepatocytes, but we did not observe ADRP distribution in the iLD fractions by

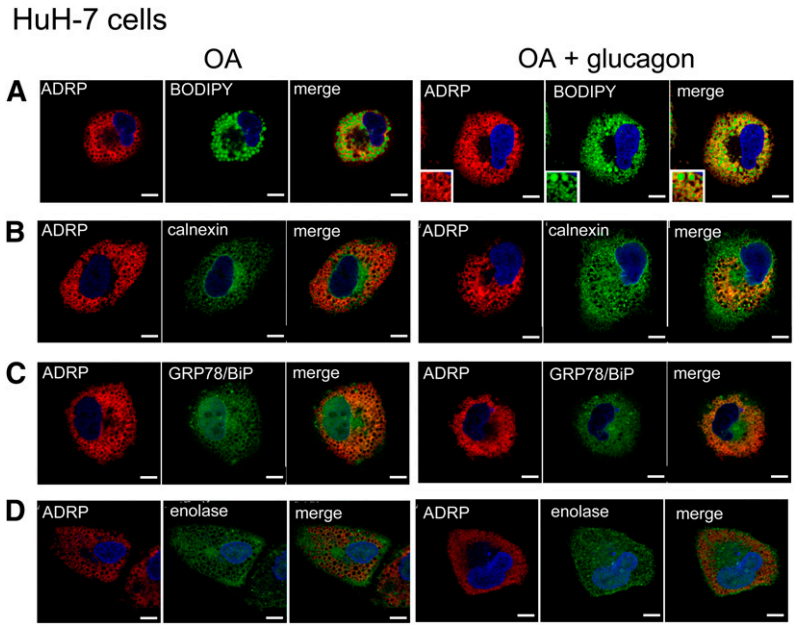

Fig. 6. Microscopic views of distribution of ADRP and other proteins in HuH-7 cells after incubation with OA or OA and glucagon. HuH-7 cells were treated with OA (0.6 mM) or with OA plus glucagon (100 nM) for 24 h. A-D: The cells were stained with anti-ADRP IgG (red) in combination with BODIPY493/503, antibodies against calnexin, GRP78/BiP, or enolase (green). The cells were also treated with DAPI to stain the nuclei (blue). The insets in (A) are enlarged images of LD particles in the HuH-7 cells treated with OA plus glucagon showing that ADRP surrounds both large and small LD particles. The cells were visualized and photographed using confocal laser microscopy. The bars indicate 10 μm. ADRP, adipose differentiation-related protein; GRP78/BiP, glucose-regulated protein of 78-kDa/binding protein; LD, lipid droplet; OA, oleic acid.

treatment of HuH-7 cells with OA alone. Therefore, we hypothesized that metabolic factors that appeared under the fasting conditions would be responsible for such a response in the liver. It is an interesting finding that glucagon induces the distribution of ADRP to the iLD fractions, but it did not increase ADRP expression. As glucagon has a pivotal role in switching body energy sources between glucose and fatty acids, iLD formation might be involved in energy homeostasis by the formation of LDs and accumulation of TG in the liver when the availability of glucose is decreased.

The glucagon receptor has seven membrane-spanning domains and is coupled with Gs-type GTP binding protein, which suggests that a PKA-dependent pathway is involved in ADRP association with the iLD fractions. Experiments with db-cAMP, a nonhydrolyzable analog of cAMP, and two PKA inhibitors clearly indicated that the distribution of ADRP to the iLD fractions is mediated by PKA. However, a recent study reported that the glucagon receptor is also coupled with Gq (36). The PLC inhibitor U-73122 also abolished the effect of glucagon, suggesting that both the PKA and PLC pathways are required for the ADRP behavior. It was reported that platelet-activating factor-induced LD formation in human polymorpholeukocytes was inhibited by U-73122 (42, 43). While the mechanism of LD formation in leukocytes might be difficult to compare with that of hepatocytes, it is possible that there is a PLC-dependent pathway that leads to iLD fraction formation.

It is well known that perilipin, the major LD protein in adipocytes, is a good substrate for PKA phosphorylation; however, ADRP does not have a phosphorylation site based on the amino acid sequence. Therefore, it is unlikely that ADRP is phosphorylated by PKA and/or PKC upon activation of hepatic cells by glucagon. It is possible that certain regulatory proteins phosphorylated by PKA and/or PKC are involved in the generation of the iLD fractions.

Massive lipid accumulation is observed in certain pathological conditions of the liver. Recently, NASH has gathered considerable attention because it is a manifestation of metabolic syndrome in the liver, and many patients suffer from it. Treatment of rodents with an MCD diet for a short period of time induces severe accumulation of lipids in the liver, which provides an animal model of NASH (28, 29).

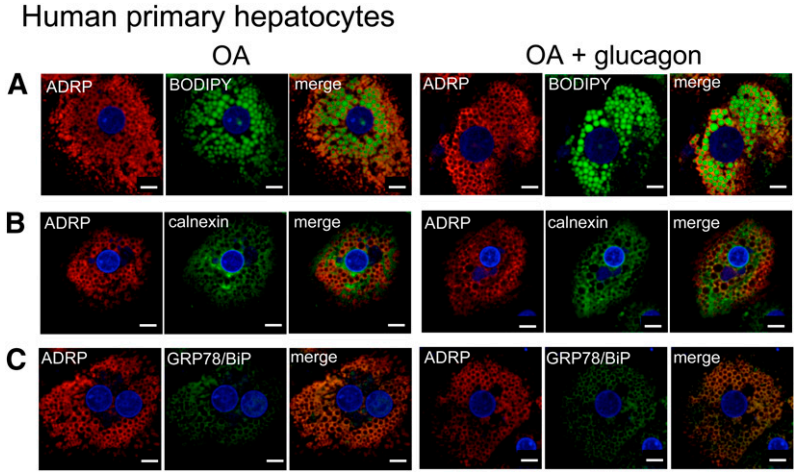

Fig. 7. Microscopic views of distribution of ADRP and other proteins in human primary hepatocytes after incubation with OA or OA and glucagon**.** Human primary hepatocytes were treated with OA (0.6 mM) or with OA plus glucagon (100 nM) for 24 h. A-D: The cells were stained with anti-ADRP IgG (red), in combination with BODIPY493/503, anti-calnexin, or anti-GRP78/BiP antibodies (green) as in the Fig. 6. The cells were also treated with DAPI to stain the nuclei (blue). The cells were visualized and photographed using confocal laser microscopy. The bars indicate 10 μm. ADRP, adipose differentiation-related protein; GRP78/BiP, glucose-regulated protein of 78-kDa/binding protein; OA, oleic acid.

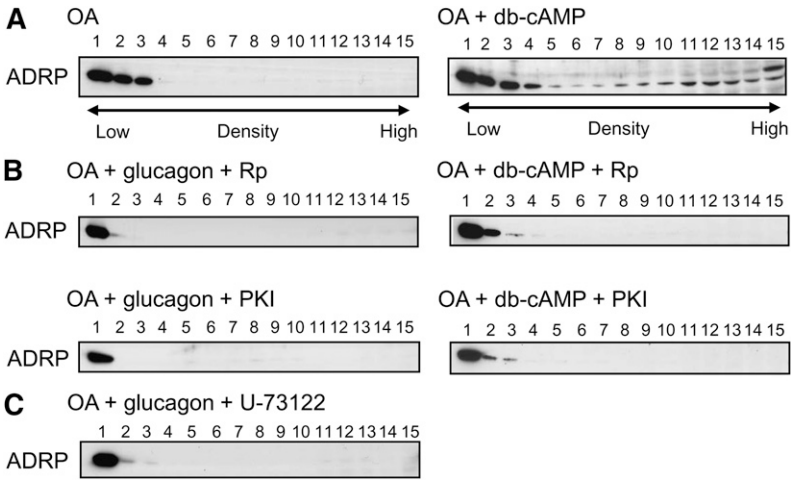

Fig. 8. ADRP appearance in iLD fractions was induced by PKA- and PLC-dependent pathways in HuH-7 human hepatoma cells. A: HuH-7 cells were incubated with 0.6 mM OA and with or without 100 μM dibutyryl cAMP (db-cAMP) for 24 h. Then the cell lysate was fractionated by sucrose ultracentrifugation, and the distribution of ADRP was detected. B: HuH-7 cells were incubated with 0.6 mM OA plus 100 nM glucagon or 100 μM db-cAMP to induce redistribution of ADRP to the iLD fraction. In addition, a PKA inhibitor, either Rp (20 μM) or PKI (50 nM), was added to the cells during the 24 h incubation. B: HuH-7 cells were incubated with 0.6 mM OA plus 100 nM glucagon to induce redistribution of ADRP to the iLD fraction. In addition, the PLC inhibitor U-73122 (5 μM) was added to the cells during the 24 h incubation. ADRP, adipose differentiation-related protein; GRP78/BiP, glucose-regulated protein of 78-kDa/binding protein; iLD, intermediate-density lipid droplet; OA, oleic acid; PKA, protein kinase A; PKI, PKI14-22amide; PLC, phospholipase C; Rp, Rp-8-Br-cAMPS.

Methionine and choline in the diet are critical nutrients to generate phosphatidylcholine (PC), and in the liver a large amount of PC is needed to assemble VLDL particles, followed by VLDL secretion (44). We found that ADRP was induced more than 4-fold along with an accumulation of TG in the liver of MCD mice. Interestingly, the subcellular distribution of ADRP in the MCD liver was quite similar to that in the liver of fasted mice, where a significant part of ADRP appeared in the iLD particles. Recently, Motomura et al. reported that ADRP was upregulated in liver steatosis in humans (45). They also demonstrated the induction of ADRP in the mouse liver after treatment with a high-fat diet (82% fat by calories) for up to 12 weeks. It is interesting that the induction of ADRP-positive iLD fractions during lipid accumulation in the liver could be a common response in both physiological and pathological conditions. However, more work is needed to clarify the mechanism for induction of ADRP-positive iLD fractions in the NASH liver.

In conclusion, we suggest that the ADRP-positive iLD fractions are formed in hepatic cells during lipid storage. In addition, we suggest that the induction and distribution of ADRP are regulated differently. The distribution of ADRP is mediated by PKA and/or PLC. Further study on the nature of iLD particles as intracellular components is certainly needed and would provide an informative aspect on formation and function of LDs.

REFERENCES

1. Murphy, S., S. Martin, and R. G. Parton. 2009. Lipid droplet-organelle interactions; sharing the fats. *Biochim. Biophys. Acta.* **1791:** 441–447.
2. Brown, D. A. 2001. Lipid droplets: proteins floating on a pool of fat. *Curr. Biol.* **11:** R446–R449.
3. Thiele, C., and J. Spandl. 2008. Cell biology of lipid droplets. *Curr. Opin. Cell Biol.* **20:** 378–385.
4. Liu, P., Y. Ying, Y. Zhao, D. I. Mundy, M. Zhu, and R. G. W. Anderson. 2004. Chinese hamster ovary K2 cell lipid droplets appear to be metabolic organelles involved in membrane traffic. *J. Biol. Chem.* **279:** 3787–3792.
5. Fujimoto, Y., H. Itabe, J. Sasaki, M. Makita, J. Noda, M. Mori, Y. Higashi, S. Kojima, and T. Takano. 2004. Identification of major proteins in the lipid droplet-enriched fraction isolated from the human hepatocyte cell line HuH7. *Biochim. Biophys. Acta.* **1644:** 47–59.
6. Brasaemle, D. L., G. Dolios, L. Shapiro, and R. Qang. 2004. Proteomic analysis proteins associated with lipid droplets of basal and lipolytically stimulated 3T3–L1 adipocytes. *J. Biol. Chem.* **279:** 46835–46842.
7. Londos, C., D. L. Brasaemle, C. J. Schultz, J. P. Segrest, and A. R. Kimmel. 1999. Perilipins, ADRP, and other proteins that associate with intracellular neutral lipid droplets in animal cells. *Semin. Cell Dev. Biol.* **10:** 51–58.
8. Wolins, N. E., B. K. Quaynor, J. R. Skinner, M. J. Schoenfish, A. Tzekov, and P. E. Bickel. 2005. S3–12, Adipophilin, and TIP47 package lipid in adipocytes. *J. Biol. Chem.* **280:** 19146–19155.
9. Londos, C., C. Sztalryd, J. T. Tansey, and A. R. Kimmel. 2005. Role of PAT proteins in lipid metabolism. *Biochimie.* **87:** 45–49.
10. Yamaguchi, T., S. Matsushita, K. Motojima, F. Hirose, and T. Osumi. 2006. MLDP, a novel PAT family protein localized to lipid droplets and enriched in the heart, is regulated by peroxisome proliferator-activated receptor alpha. *J. Biol. Chem.* **281:** 14232–14240.
11. Sztalryd, C., G. Xu, H. Dorward, J. T. Tansey, J. A. Contreras, A. R. Kimmel, and C. Londos. 2003. Perilipin A is essential for the translocation of hormone-sensitive lipase during lipolytic activation. *J. Cell Biol.* **161:** 1093–1103.
12. Martinez-Botas, J., J. B. Anderson, D. Tessier, A. Lapillonne, B. H-J. Chang, M. J. Quast, D. Gorenstein, K-H. Chen, and L. Chan. 2000. Absence of perilipin results in leanness and reverses obesity in Lepr(db/db) mice. *Nat. Genet.* **26:** 474–479.
13. Brasaemle, D. L. 2007. The perilipin family of structural lipid droplet proteins: stabilization of lipid droplets and control of lipolysis. *J. Lipid Res.* **48:** 2547–2559.

14. Watt, M. J., and G. R. Steinberg. 2008. Regulation and function of triacylglycerol lipases in cellular metabolism. *Biochem. J.* **414:** 313–325.
15. Yamaguchi, T., N. Omatsu, S. Matsushita, and T. Osumi. 2004. CGI-58 interacts with perilipin and is localized to lipid droplets. Possible involvement of CGI-58 mislocalization in Chanarin-Dorfman syndrome. *J. Biol. Chem.* **279:** 30490–30497.
16. Jiang, H. P., and G. Serrero. 1992. Isolation and characterization of a full-length cDNA coding for an adipose differentiation-related protein. *Proc. Natl. Acad. Sci. USA.* **89:** 7856–7860.
17. Russell, T. D., C. A. Palmer, D. J. Orlicky, A. Fischer, M. C. Rudolph, M. C. Neville, and J. L. McManaman. 2007. Cytoplasmic lipid droplet accumulation in developing mammary epithelial cells: roles of adiopophilin and lipid metabolism. *J. Lipid Res.* **48:** 1463–1475.
18. Mishra, R., S. N. Emancipator, C. Miller, T. Kern, A. Hill, and M. S. Simonson. 2004. Adipose differentiation-related protein and regulators of lipid homeostasis identified by gene expression profiling in the murine *db/db* diabetic kidney. *Am. J. Physiol. Renal Physiol.* **286:** F913–F921.
19. Vosper, H., L. Patel, T. L. Graham, G. A. Khoudoli, A. Hill, C. H. Macphee, I. Pinto, S. A. Smith, K. E. Suckling, C. R. Wolf, et al. 2001. The peroxisome proliferator-activated receptor δ promotes lipid accumulation in human macrophages. *J. Biol. Chem.* **276:** 44258–44265.
20. Dalen, K. T., S. M. Ulven, B. M. Arntsen, K. Solaas, and H. I. Nebb. 2006. PPARα activators and fasting induce the expression of adipose differentiation-related protein in liver. *J. Lipid Res.* **47:** 931–943.
21. Masuda, Y., H. Itabe, M. Odaki, K. Hama, Y. Fujimoto, M. Mori, N. Sasabe, J. Aoki, H. Arai, and T. Takano. 2006. ADRP/adipophilin is degraded through the proteasome-dependent pathway during regression of lipid-storing cells. *J. Lipid Res.* **47:** 87–98.
22. Schaiff, W. T., M. G. Carlson, S. D. Smith, R. Levy, D. M. Nelson, and Y. Sadovsky. 2000. Peroxisome proliferator-activated receptor-γ modulates differentiation of human trophoblast in a ligand-specific manner. *J. Clin. Endocrinol. Metab.* **85:** 3874–3881.
23. Suzuki, K., K. Takahashi, T. Nishimaki-Mogami, H. Kagechika, M. Yamamoto, and H. Itabe. 2009. Docosahexaenoic acid induces adipose differentiation-related protein through activation of retinoid X receptor in human choriocarcinoma BeWo cells. *Biol. Pharm. Bull.* **32:** 1177–1182.
24. Edvardsson, U., A. Lungberg, D. Linden, L. William-Olsson, H. Peilot-Sjogren, A. Ahnmark, and J. Oscarsson. 2006. PPARα activation increases triglyceride mass and adipose differentiation-related protein in hepatocytes. *J. Lipid Res.* **47:** 329–340.
25. Gao, J., and G. Serrero. 1999. Adipose differentiation-related protein (ADRP) expressed in transfected COS-7 cells selectively stimulates long chain fatty acid uptake. *J. Biol. Chem.* **274:** 16825–16830.
26. Paul, A., B. H-J. Chang, L. Li, V. K. Yechoor, and L. Chan. 2008. Deficiency of adipose differentiation-related protein impairs foam cell formation and protects against atherosclerosis. *Circ. Res.* **102:** 1492–1501.
27. Xu, G., C. Sztalryd, X. Lu, J. T. Tansey, J. Gan, H. Dorward, A. R. Kimmel, and C. Londos. 2005. Post-translational regulation of adipose differentiation-related protein by the ubiquitin/proteasome pathway. *J. Biol. Chem.* **280:** 42841–42847.
28. Kirsch, R., V. Clarkson, E. G. Shephard, D. A. Marais, M. A. Jaffer, V. E. Woodburne, R. E. Kirsch, and P. L. Hall. 2003. Rodent nutritional model of non-alcoholic steatohepatitis: species, strain and sex difference studies. *J. Gastroenterol. Hepatol.* **18:** 1272–1282.
29. Leclercq, I. A., G. C. Farrell, J. Field, D. R. Bell, F. J. Gonzalez, and G. R. Robertson. 2000. CYP2E1 and CYP4A as microsomal catalysts of lipid peroxides in murine nonalcoholic steatohepatitis. *J. Clin. Invest.* **105:** 1067–1075.
30. Gibbons, G. F., K. Islam, and R. J. Pease. 2000. Mobilization of triacylglycerol stores. *Biochim. Biophys. Acta.* **1483:** 37–57.
31. Carmen, G. Y., and S. M. Victor. 2006. Signaling mechanisms regulating lipolysis. *Cell. Signal.* **18:** 401–408.
32. Wolins, N. E., B. K. Quaynor, J. R. Skinner, A. Tzekov, M. A. Croce, M. C. Gropler, V. Varma, A. Yao-Borengasser, N. Rasouli, P. A. Kern, et al. 2006. OXPAT/PAT-1 is a PPAR-induced lipid droplet protein that promotes fatty acid utilization. *Diabetes.* **55:** 3418–3428.
33. Cho, S. Y., E. S. Shin, P. J. Park, D. W. Shin, H. K. Chang, D. Kim, H. H. Lee, J. H. Lee, S. H. Kim, M. J. Song, et al. 2007. Identification of mouse Prp19p as a lipid droplet-associated protein and its possible involvement in the biogenesis of lipid droplets. *J. Biol. Chem.* **282:** 2456–2465.
34. Higashi, Y., H. Itabe, H. Fukase, M. Mori, and Y. T. Takano. 2003. Transmembrane lipid transfer is crucial for providing neutral lipids during VLDL assembly in endoplasmic reticulum. *J. Biol. Chem.* **278:** 21450–21458.
35. Sato, S., M. Fukasawa, Y. Yamakawa, T. Natsume, T. Suzuki, I. Shoji, H. Aizaki, T. Miyamura, and M. Nishijima. 2006. Proteomic profiling of lipid droplet proteins in hepatoma cell lines expressing hepatitis C virus core protein. *J. Biochem.* **139:** 921–930.
36. Jiang, G., and B. B. Zhang. 2003. Glucagon and regulation of glucose metabolism. *Am. J. Physiol. Endocrinol. Metab.* **284:** E671–E678.
37. Ohsaki, Y., J. Cheng, M. Suzuki, A. Fujita, and T. Fujimoto. 2009. Lipid droplets are arrested in the ER membrane by tight binding of lipidated apolipoprotein B-100. *J. Cell Sci.* **121:** 2415–2422.
38. Ohsaki, Y., J. Chen, M. Suzuki, Y. Shinohara, A. Fujita, and T. Fujimoto. 2009. Biogenesis of cytoplasmic lipid droplets: From the lipid ester globule in the membrane to the visible structure. *Biochim. Biophys. Acta.* **1791:** 399–407.
39. Ye, J., J. Z. Li, Y. Liu, X. Li, T. Yang, X. Ma, Q. Li, Z. Yao, and P. Li. 2009. Cideb, an ER- and lipid droplet-associated protein, mediates VLDL lipidation and maturation by interacting with apolipoprotein B. *Cell Metab.* **9:** 177–190.
40. Turró, S., M. Ingelmo-Torres, J. M. Estanyol, F. Tebar, M. A. Fernández, C. V. Albor, K. Gaus, T. Grewal, C. Enrich, and A. Pol. 2006. Identification and characterization of associated with lipid droplets protein 1: a novel membrane-associated protein that resides on hepatic lipid droplets. *Traffic.* **7:** 1254–1269.
41. Robenek, H., O. Hofnagel, I. Buers, M. J. Robenek, D. Troyer, and N. J. Severs. 2006. Adipophilin-enriched domains in the ER membrane are sites of lipid droplet biogenesis. *J. Cell Sci.* **119:** 4215–4224.
42. Bozza, P. T., J. L. Payne, J. L. Goulet, and P. F. Weller. 1996. Mechanisms of platelet-activating factor-induced lipid body formation: requisite roles for 5-lipoxygenase and de novo protein synthesis in the compartmentalization of neutrophil lipids. *J. Exp. Med.* **183:** 1515–1525.
43. Bozza, P. T., K. G. Magalhães, and P. F. Weller. 2009. Leukocyte lipid bodies: biogenesis and functions in inflammation. *Biochim. Biophys. Acta.* **1791:** 540–551.
44. Nishimaki-Mogami, T., Z. Yao, and K. Fujimori. 2002. Inhibition of phosphatidylcholine synthesis via the phosphatidylethanolamine methylation pathway impairs incorporation of bulk lipids into VLDL in cultured rat hepatocytes. *J. Lipid Res.* **43:** 1035–1045.
45. Motomura, W., M. Inoue, T. Ohtake, N. Takahashi, M. Nagamine, S. Tanno, Y. Kohgo, and T. Okumura. 2006. Up-regulation of ADRP in fatty liver in human and liver steatosis in mice fed with high fat diet. *Biochem. Biophys. Res. Commun.* **340:** 1111–1118.